JNEST EISSN: 2961-8738 ● PISSN: 2961-8916 ● DOI: 10.56741/jnest.v3i02.525
Article Received 9 February 2024. Revised 30 March 2024.

Analysis of Third-Generation Solar Cell Design with Physics of Semiconductor

Hsu Myat Tin Swe*, Ei Ei Khin, Khaing Thandar Soe, Lei Lei Yin Win, Hla Myo Tun, Devasis Pradhan

***Abstract*—The paper presents the Analysis of Generation Solar Cell Design with Physics of Semiconductor. The research problem in this study is how to design a high-performance solar cell with novel semiconductor compounds that are fabricated in the laboratory based on the physical parameters. The approach to solving the proposed research problem is based on experimental studies through theoretical research in recent works. The first one is to develop the effective structure for solar cell design and the other is to develop the energy band structure of III-V compound-based third-generation solar cell. The simulation analyses were carried out with the help of MATLAB language. There are many steps to designing high-performance semiconductor devices for real-world applications. The results confirm that the numerical analyses of these two developments could be supported to estimate the outcomes of experimental studies without using real equipment in the laboratory.**

***Index Terms*— Design, Semiconductor, Solar Cell, Third Generation**

I. INTRODUCTION

A quantum-well is one of the semiconductor nanostructures. In a quantum-well structure, a narrow band-gap material is sandwiched between wider band-gap materials. Quantum wells can make to improve the output power of light, recombination rate, carrier injection efficiency, and so on. There are two basic types of quantum well design for solar cell fabrication. They are (i) Type-I: the charge carriers are localized in the same layer (fast recombination), and (ii) Type-II: the charge carriers are localized in different layers (long-time recombination) [1-3].

As for recent solar cells in the research field, the energy conversion efficiency has been improved to approximately 45 %, while the improvement in the light–electric energy conversion efficiency is only a few percent in the past ten years. Now the mainstream in research to improve the energy conversion efficiency is the optimization of stacking structures of three or four cells by allocating three or four light wavelength ranges to the respective cells.

The performance comparison between GaN and Si had been done with the Optical Power. The Output Optical Power of GaN is higher than that of Si. The high-performance solar cell could be utilized with GaN Materials instead of Si Material in reality. Figure.1. shows the Performance Comparison Results for GaN and Si [4-6].

Hsu Myat Tin Swe (Corresponding author)**, Ei Ei Khin, Khaing Thandar Soe, and Lei Lei Yin Win** are with Department of Electronic Engineering, Yangon Technological University, Gyogone, Insein PO, 11011, Yangon, Myanmar. **Hla Myo Tun** is with Department of Research, Yangon Technological University, Gyogone, Insein PO, 11011, Yangon, Myanmar. **Devasis Pradhan** is Department of Electronic and Communication Engineering, Acharya Institute of Technology, India. Correspondence: ecdepartment.ytu@gmail.com

Some recent works regarding the Different hole transport layers (HTLs) have also been reported and selected to address the mismatching energy band alignment at the perovskite/HTL interface.

The fundamental concepts of solar cells are learned by using the absorbing properties of the sunlight. The light can be reflected at the interface between the sun-facing surface of the solar cell device and the air or at the interface between the solar cell's layers. Thus, some of the incident light that contributes to the conversion efficiency of solar cells can be affected by this reflection. This is especially a problem for heterojunction devices [9-12].

The research objectives of this study are to focus on the novel solar cell structure for higher efficiency achievement and to analyze the physical parameters for designing and modeling the solar cell design.

The paper is organized as follows. Section II presents the material and method for the proposed solar cell model. Section III mentions the implementation of the proposed solar cell structure. Section IV gives the theoretical results with numerical analyses. Section V concludes the outcomes of the research.

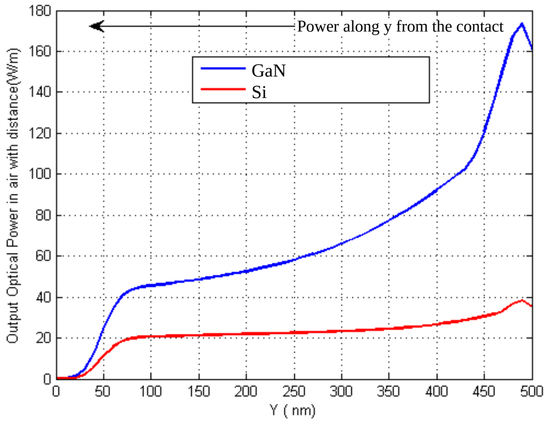

Fig. 1. Performance Comparison Results for GaN and Si

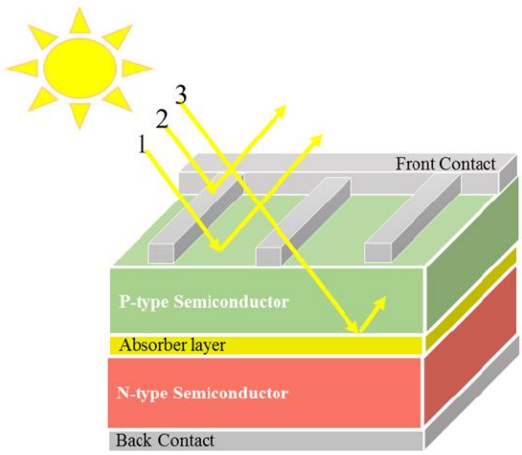

Fig. 2. Illustrates the fundamental concepts

II. MATERIALS AND METHODS

A. *Solar Radiation and Basic Device Parameters*

The illumination is given in AMX (air mass X) where

$$X = \frac{1}{\cos\theta} \quad (1)$$

and θ is the angle between the zenith and the position of the sun under terrestrial conditions. Air mass zero (AM0) is the solar irradiation above the earth's atmosphere. The accepted standard for AM0 is 135.3 mW/cm^2 or 1.353 kW/m^2, which is known as the solar constant. Air mass one (AM1) is when the sun is directly overhead and about 70% of the sunlight incident on the earth's atmosphere reaches the earth's surface on a clear day. The rest is absorbed or backscattered. AM2 is when the sun is at 60° from the zenith. AM1.5 is when the sun is at 48.19° from the zenith [13-18].

B. *Ideal Conversion Efficiency*

The current versus the bias voltage of a p-n junction in the presence of light illumination is the same as what we have derived for a photodiode,

$$I = I_0\left(e^{qV/\gamma k_B T} - 1\right) - I_{ph} \quad (2)$$

C. *p-n Junction Solar Cells and Spectral Response*

Fig. 3 shows the schematics of an n-on-p solar cell, where the solar light illumination is from the top surface with an antireflection coating to improve photon collection, and the electrode fingers are for current collection [19-20].

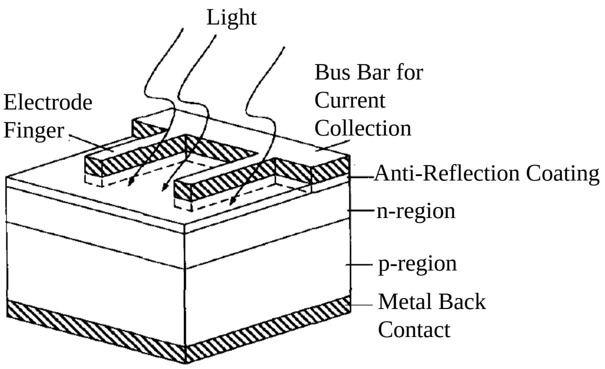

(a) Device Design for Solar Cell

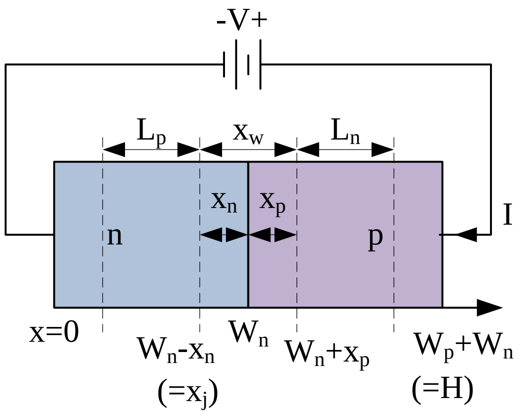

(b) Equivalent Circuit Model

Fig. 3. Schematic Solar Cell Structure

D. *Generation Rate Model*

The generation rate of electron-hole pairs is proportional to the optical intensity profile in the device

$$G(x,\lambda) = G_0 e^{-\alpha(\lambda)x}$$
$$G_0 = \eta_i\left[1 - R(\lambda)\right]\Phi(\lambda)\alpha(\lambda) \quad (3)$$

where α(λ) is the absorption spectrum, Φ(λ) is the optical flux density for an incident optical power intensity ηi is the intrinsic quantum efficiency to account for the average number (100% maximum) of electron-hole pairs generated per incident photon.

III. IMPLEMENTATION

A. *Harmonic Oscillator Potential and Wavefunctions*

The Schrodinger equation is an outstanding mathematical model for analyzing the harmonic oscillator.

$$-\frac{\hbar^2}{2m}\frac{d^2\psi_n(x)}{dx^2} + \frac{1}{2}m\omega^2 x^2\psi_n(x) = E_n\psi_n(x) \quad (4)$$

Where
n=wavefunctions
m is the vibrating mass
ω is the natural vibration frequency related to the spring stiffness constant C

$$-\frac{d^2\psi_n(y)}{dy^2} + y^2\psi_n(y) = \varepsilon_n\psi_n(y) \quad (5)$$

$$\psi_n(y) = A_n H_n(y)\exp\left(-\frac{y^2}{2}\right), \varepsilon_n = 2n+1, \quad (6)$$

$$A_n = \left(\frac{1}{n!2^n\sqrt{\pi}}\right)^{\frac{1}{2}} \quad (7)$$

$$E_n = \left(n + \frac{1}{2}\right)\hbar\omega \quad (8)$$

B. *Group and Phase Velocity*

The phase velocity is v_{ph} = ω/k = 17.674m/s, while the envelope moves with v_G = dω/dk = 0.833m/s.

$$y_i(x,t) = A\sin\left(k_i x - \omega_i t\right) \quad (9)$$

$$v_{ph} = -\frac{\left(\partial\phi/\partial t\right)\big|_x}{\left(\partial\phi/\partial t\right)\big|_t} \quad (10)$$

$$y_i(x,t) = 2A\cos\left[\delta k\left(x - v_G t\right)\right]\sin\left(kx - \omega t\right) \quad (11)$$

$$\vec{v}_G = \vec{\nabla}_k\omega(\vec{k}) \quad (12)$$

where
y_1=Phase Velocity
y_2=Group Velocity

C. *Oscillator Chain Model*

The model in this section is the oscillator chain model for quantum well structure. Equation (12) to Equation (14) could be utilized to analyze the oscillation with different time steps in Fig. 9. If the time steps are changing from the initial point to the final point, the chain of oscillation could be observed from the half cycles of the sinusoidal signal because of the variation of the well width and different wavefunctions in reality.

$$y_{i,p}(t=0) = A\sin\left(K_p x_i\right) \quad (12)$$

for the ith atom located at

$$x_i = ia \text{ for } 0 \le i \le N \qquad (13)$$

in the pth vibrational mode with Kp given by

$$A = 1\dot{A} \qquad (14)$$

D. Phonon Velocity Vs Temperature (Debye T^3 Law)

The important consideration for phonon velocity concerning temperature could be analyzed by using the Debye T^3 Law.

$$U_{lowT} \approx 9Nk_B T \left(\frac{T}{\theta}\right)^3 \int_0^\infty dx \frac{x^3}{\left[e^x - 1\right]} \qquad (15)$$

$$U_{lowT} \approx 9Nk_B T \left(\frac{T}{\theta}\right)^3 \frac{6\pi^4}{90} = \frac{3\pi^4 Nk_B T^4}{5\theta^3} \qquad (16)$$

The low-temperature expression for the heat capacity of the solid can be obtained by taking d/dT of U_{lowT}, to get

$$C_{VlowT} \approx \frac{12\pi^4 Nk_B T^3}{5\theta^3} \sim 233.78 Nk_B \left(\frac{T}{\theta}\right)^3 \qquad (17)$$

The evaluation of the general form of U has to be done numerically and the results with its low and high-temperature behaviors. Notice how well the Debye T^3 law describes the low-temperature behavior of C_V.

E. I-V Characteristics of 3rd Generation Solar Cell (Mathematical Model)

The VI characteristics of third-generation solar cells with mathematical models could be utilized as follows:

$$I = I_0\left(e^{qV_A/kT} - 1\right) \qquad (18)$$

$$I_0 = qA\left(\frac{D_N}{L_N}\frac{n_i^2}{N_A} + \frac{D_P}{L_P}\frac{n_i^2}{N_D}\right) \qquad (19)$$

F. Fill Factor Analysis for Solar Cell

The ratio between the product of current and voltage at the maximum power point to the product of short circuit current and open circuit voltage of the solar cell.

$$Fill\ Factor = \frac{P_m}{I_{sc} \times V_{oc}} \qquad (20)$$

The fill factor of the solar cell could be observed at the intersection between open circuit voltage and short circuit current during the absorption of the solar ray in the application.

III. RESULTS AND DISCUSSIONS

A. Depletion Width Estimation in Conventional Solar Cell Structure to High-Performance Solar Cell Design with Physical Parameters

1. Spectral Irradiance vs. hv

The solar radiation spectrum for various conditions. Air mass zero (AMO) is the solar irradiation above the earth's atmosphere (= 135.3 mW/cm^2, also known as solar constant) [21],[22]. It follows close to the black body radiation of a 5800K source from the sun's surface. The dataset comes from the National Renewable Energy Laboratory – NREL.

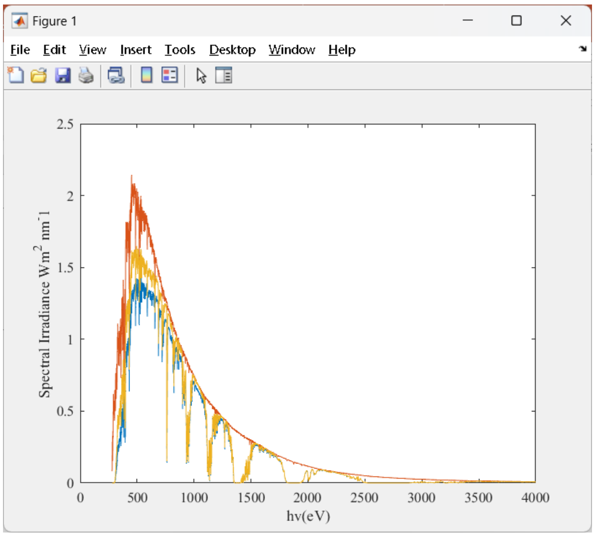

Fig. 4. Result of Spectral Irradiance Vs hv

2. Generation Rate of Electron-Hole Pairs

The generation rate of electron-hole pairs is a function of the optical penetration distance into the semiconductor p-n junction.

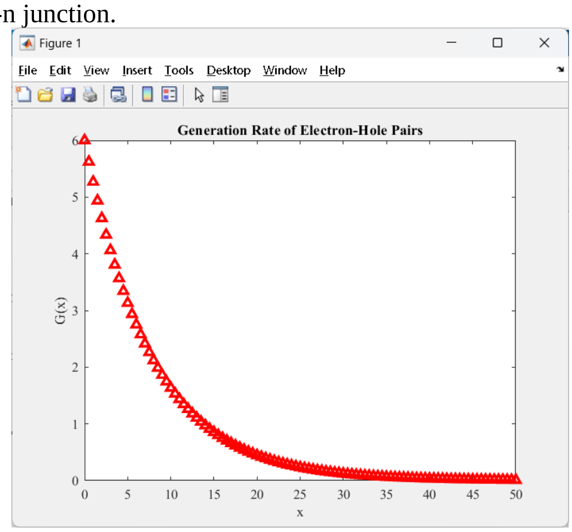

Fig. 5. Result of Generation of Electron-Hole Pairs

3. Results of Depletion Width Calculation

The depletion width depends on the acceptor and donor concentration. If the carrier concentration and applied voltage are increased, the depletion width could be narrow.

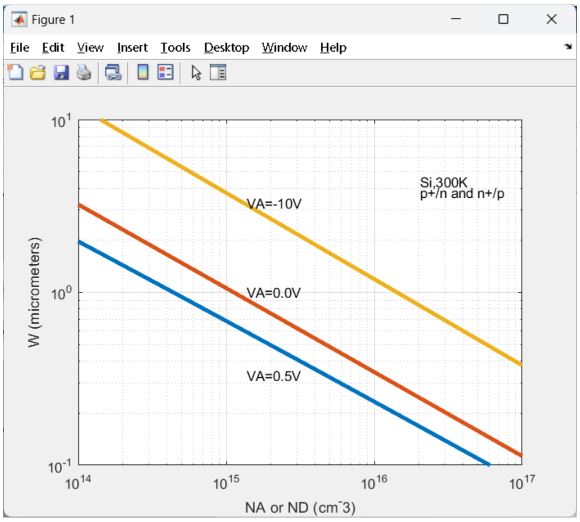

Fig. 6. Depletion Width Calculation Results

Based on the dataset from the National Renewable Energy Laboratory – NREL, the spectral irradiance could be observed for targeting the efficiency. According to the physics of solar cells, the p-n junction solar cells and spectral response show the generation rate for electron and hole pairs in the solar cells. The generation rate could decay after increasing the optical penetration distance into the p-n junction. The energy band diagram is the critical observation between p-n junction solar cells. The observation from the energy band diagram and the quasi-Fermi levels for a small forward bias voltage could extend the quantum well structure for high-performance conditions.

B. Harmonic Oscillator Potential and Wavefunctions

Fig. 7 illustrates the Harmonic Oscillator Potential and Wavefunctions. The number of wavefunctions depends on the oscillation in the quantum well structure.

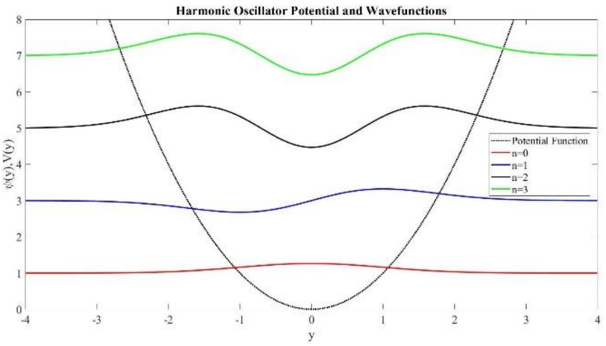

Fig. 7. Harmonic Oscillator Potential and Wavefunctions

Vibrations in crystals are quantized and are known as phonons. Whereas a photon is a quantum of light, a phonon is a quantized crystal vibration. The first four wavefunctions along with their associated energy levels were observed to understand the phonon in a crystal. Two waves $y_1(x, t)$ and $y_2(x, t)$ are superimposed to obtain the resulting wave yt (x, t). The parameters used for the waves are A = 1, ω_1 = 51.0Hz, k_1 = 3.0 m^{-1}, ω_2 = 50.8Hz, k_2 = 2.76 m^{-1}, with phase velocities $v_{ph1} = \omega_1/k_1$ = 17.0m/s, $v_{ph2} = \omega_2/k_2$ = 18.406m/s. The resulting wave has ω = 50.9Hz, k = 2.88 m^{-1}, dω = 0.1Hz = $\delta\omega$, and dk = 0.12 m^{-1} = δk.

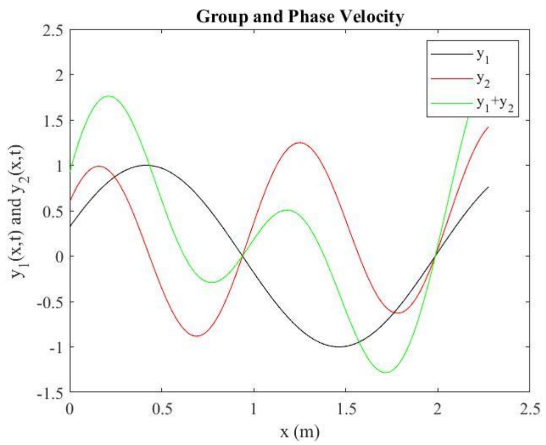

Fig. 8. Results of Group and Phase Velocity

Fig. 8 shows the Results of Group and Phase Velocity.

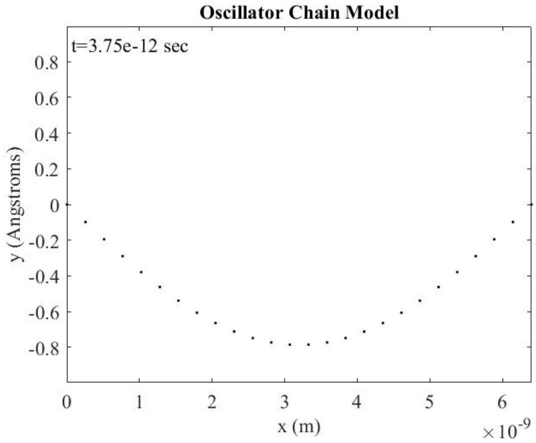

Fig. 9. Oscillation Result for Specific Time Step (Final)

Factors Affecting the limiting efficiency are very important to model the physical structure of solar cell design. The homojunction and heterojunction structures are not appropriate for third-generation solar cells. Quantum Well Structure is suitable for designing and modeling the High-performance Solar Cell Structure. The Harmonic Oscillator Potential and Wavefunctions directly affected to design of the high-performance solar cell. Figure 10 shows the Results of Phonon Velocity vs. temperature.

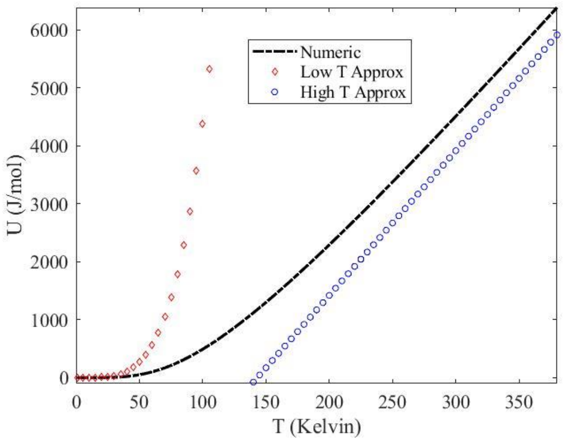

Fig. 10. Results of Phonon Velocity Vs Temperature

C. Energy Band Diagram of Quantum Well Solar Cell Design

The energy band diagram of the proposed quantum well solar cell could be observed with different thicknesses of materials. The respective band structure for different layers could be found in the energy band gap. The energy band diagram of the proposed quantum well solar cell is the measurement results of the energy efficiency such as internal and external performance.

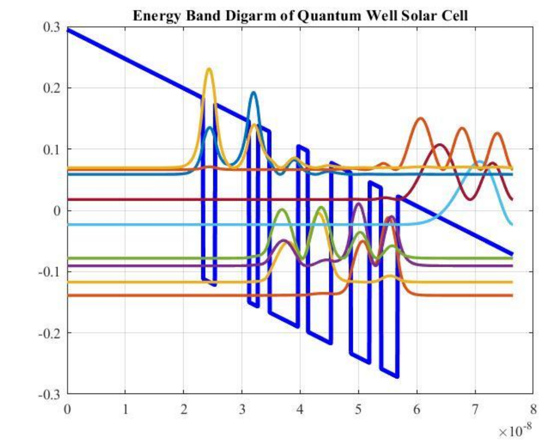

Fig. 11. Energy Band Diagram of Quantum Well Solar Cell Design

D. J-V Characteristics of 3rd Generation Solar Cells with Different Thickness

As the same optoelectronics properties have been used to simulate the diffusion constant, mobility, and surface recombination velocity for both electron and hole, so the same results have been achieved for both conditions. However, the variation of efficiencies is due to the intensity of incident irradiance and the input power of 3rd Generation Solar Cells. The theoretical efficiencies of different values of thickness conditions have been simulated as 46% and above under one sun condition.

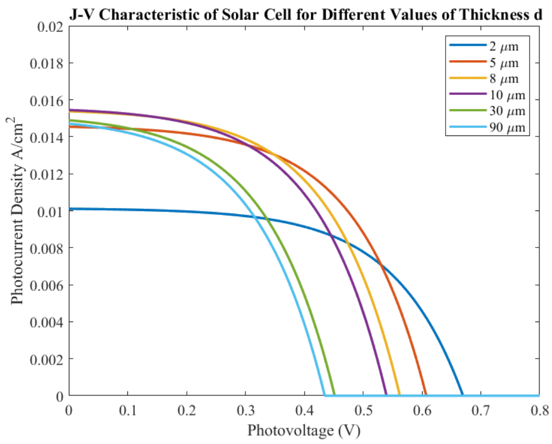

Fig.12. J-V Characteristics of 3rd Generation Solar Cells with Different Thickness

E. I-V Characteristics of 3rd Generation Solar Cell

For reverse bias greater than a few kT/q, a few tenths of a volt at room temperature, the exponential voltage term in the idea solar cell equation becomes negligible and I➔-I_0. According to the ideal solar cell theory, this saturation current would be observed for reverse voltages of unlimited magnitude. For forward biasing greater than a few kT/q, the exponential term dominates, and I➔I_0=exp(qV_A/kT). If the ratio of I/I_0 is increased, the value of V_A could be increased instantly.

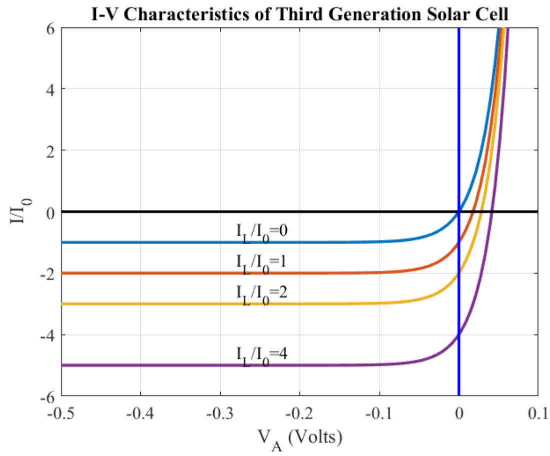

Fig. 13. I-V Characteristics of 3rd Generation Solar Cell

The fill factor corresponds to the efficiency of the solar cell and it is considered that the radiation power on the earth is about 1000 watts/square meter hence if the exposed surface area of the cell is A then the total radiation power on the cell will be 1000 watts.

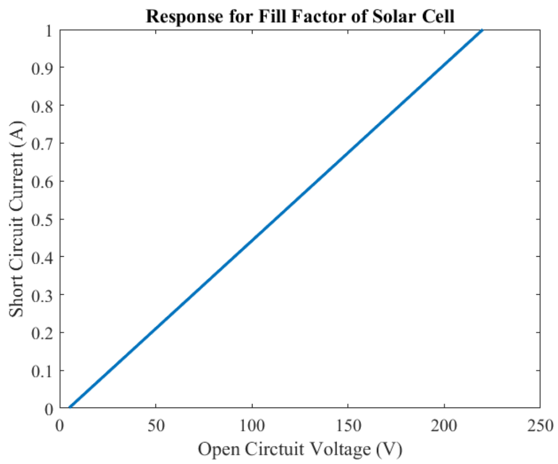

Fig. 14. Fill Factor Results for Solar Cell

IV. CONCLUSION

We use Gallium atoms equidistantly displaced from each other by the lattice constant a. We take the initial distribution as y_A*sin[j*pi/L], where L=N*a is the initial distribution of particles. Use M=1.05e-25kg for the mass of a Gallium atom, and simulate for a short time enough to determine the oscillation period from which ω can be determined. The number of orbitals per energy versus energy as the product of the 3-Dim dos times the Fermi-Dirac distribution function is plotted versus energy. The evaluation of the general form of U has to be done numerically and the results with its low and high-temperature behaviors. Notice how well the Debye T^3 law describes the low-temperature behavior of C_V. According to the physics of solar cell design, the Quantum Well structure is a very efficient design for modeling the high-performance solar cell. The important consideration for matching in the Single Quantum Well Energy Band could be analyzed with various wavefunctions (n=1,2, and 3). Single quantum well solar cells will be analyzed based on the various conditions to meet the high-performance results based on the physical parameters. Quantum well solar cells have been analyzed based on the various conditions to meet the high-performance results based on the physical parameters. The energy efficiency for designing quantum well solar cells could be observed based on the energy band diagram and energy band structure design for the specific measurement.

CONFLICTS OF INTEREST

The authors declare that there is no conflict of interest regarding the publication of this article.

CONTRIBUTIONS

This study mainly focuses on the wheeled mobile robot control system design based on fuzzy logic control. The theoretical analyses on mathematical modeling for the mobile robot play a vital role in enhancing the high-performance dynamical system for future autonomous vehicle technology. This work could be provided to find the solution for research problems in advanced controller design under the control system design in reality.

FUNDING

This work is partially supported by Research Funds under the Semiconductor Electronics Engineering Research Group of the Department of Electronic Engineering of Yangon Technological University.

ACKNOWLEDGMENT

The author would like to acknowledge many colleagues from the Semiconductor Electronics Engineering Research Group under the Department of Electronic Engineering of Yangon Technological University for providing the idea to complete this work- this collaborative research project with the Acharya Institute of Technology in India.

REFERENCES

[1] Villalva, M. G., Gazoli, J. R., & Ruppert Filho, E. (2009). Comprehensive approach to modeling and simulation of photovoltaic arrays. *IEEE Transactions on power electronics*, *24*(5), 1198-1208.

[2] Singh, K. J., Rajanna, K. M., Basu, S., & Sarkar, S. K. (2011). Numerical simulation model of compositionally graded optimized radiation hard InGaN multi-junction space solar cell. *Second International Conference on Sustainable Energy and Intelligent System (SEISCON 2011)*. Dr. M.G.R. University, Maduravoyal, Chennai, Tamil Nadu, India.

[3] Physical Properties of Semiconductors. Available at: www.ioffe.rssi.ru/SVA/NSM .

[4] Würfel, P., & Würfel, U. (2016). *Physics of solar cells: from basic principles to advanced concepts*. John Wiley & Sons.

[5] Green, M. A. (2000). *Power to the people: sunlight to electricity using solar cells*. UNSW Press.

[6] Fonash, S. (2010). *Solar cell device physics*. Second Edition. Elsevier Inc.

[7] M¨oller, H. J. (1993). *Semiconductors for Solar Cells*. Norwood, MA: Artech House.

[8] Fahrenbruch, A. L. & Bube, R. H. (1983). *Fundamentals of Solar Cells*. San Francisco, CA: Academic.

[9] Lasnier, F. & Ang, T. G. (1990). *Photovoltaic Engineering Handbook*. New York: Adam Hilger.

[10] – (2003). *Photovoltaic systems technology*. Universit¨at Kassel, Kassel, Germany.

[11] Castaner, L., & Silvestre, S. (2002). *Modelling photovoltaic systems using PSpice*. John Wiley and Sons.

[12] Krane, K. S. (2019). *Modern physics*. John Wiley & Sons.

[13] Guechi, A., & Chegaar, M. (2007). Effects of diffuse spectral illumination on microcrystalline solar cells. *J. Electron Devices*, *5*, 116-121.

[14] Lauffenburger, H. A., & Anderson, R. T. (1982). Reliability terminology and formulae for photovoltaic power systems. *IEEE Transactions on reliability*, *31*(3), 289-295.

[15] Chizaki, M., Oki, K., & Ishitani, Y. (2022). Effect of phononic and electron collisional interaction on temperature dependent exciton radiation dynamics of doped GaN. *Journal of Luminescence*, *243*, 118603.

[16] Lin, B., Aye, H. L. L., Imae, Y., Hayashi, K., Orito, H., Ma, B., ... & Ishitani, Y. (2022). Thermal radiation resonating with longitudinal optical phonon from surface micro-stripe structures on metal-gallium nitride and sapphire. *Materials Science in Semiconductor Processing*, *147*, 106726.

[17] Chizaki, M., Oki, K., & Ishitani, Y. (2022). Origin of temperature dependence of exciton radiative lifetime of GaN studied by phononic-excitonic-radiative model. *Materials Science in Semiconductor Processing*, *148*, 106794.

[18] Nakayama, T., Ito, K., Ma, B., Iida, D., Najmi, M. A., Ohkawa, K., & Ishitani, Y. (2022). Analysis of phonon transport through heterointerfaces of InGaN/GaN via Raman imaging using double-laser system: The effect of crystal defects at heterointerface. *Materials Science in Semiconductor Processing*, *150*, 106905.

[19] Win, P. S., Swe, H. M. T., & Tun, H. M. (2021). Computerized FDTD Method for Longitudinal Optical Phonon Energy on Semiconductor Hybrid Structure for High Power Devices Fabrication. *Journal of Computer Science Research*, *3*(2), 39-51.

[20] Tun, H. M., & Nwe, M. S. (2022, February). Fabrication of High Performance High Electron Mobility Transistor Design Based on III-V Compound Semiconductor. In *Proceedings of the 11th International Conference on Robotics, Vision, Signal Processing and Power Applications: Enhancing Research and Innovation through the Fourth Industrial Revolution* (pp. 376-381). Singapore: Springer Singapore.

[21] Tun, H. M., Wulansari, R. E., Pradhan, D., & Naing, Z. M. (2023). Design, fabrication and measurement of metal-semiconductor field effect transistor based on zinc oxide material. *Journal of Engineering Researcher and Lecturer*, *2*(3), 104-111.

[22] Tun, H. M., Pradhan, D., Behera, M., Nwe, M. S., Aye, S. M., Mon, A. T., & Naing, Z. M. (2023). Development of Square Patch Microstrip Antenna Design by Using Three Dimension Finite Difference Time Domain Methods. *Journal of Novel Engineering Science and Technology*, *2*(03), 83-88.

Dr. Ei Ei Khin is a Professor of the Department of Electronic Engineering at Yangon Technological University, Myanmar. She also manages the Remote Sensing and GIS Research Centre of Yangon Technological University. (email: maeieikhin.ytu@gmail.com).

Dr. Khaing Thandar Soe is an Assistant Lecturer at the Department of Electronic Engineering of Yangon Technological University, Myanmar. (email: makhaingthandarsoe.ytu@gmail.com).

Dr. Lei Lei Yin Win is a Professor of the Department of Electronic Engineering at Yangon Technological University, Myanmar. (email: maleileiyinwin.ytu@gmail.com).

Dr. Hla Myo Tun is a Leading Pro-Rector for Research and Engineering Higher Education at Yangon Technological University (YTU), Myanmar. He specializes in professional training for Engineering Higher Education leaders, heads of departments, and faculty members. He also directs Research and Development programs and workshops and has worked as a certified Quality Assurance Evaluator of the Myanmar Engineering Council (MEngC) since 2019. (email: kohlamyotun.ytu@gmail.com).

Mr. Devasis Pradhan is working as an Assistant Professor in Grade 1 and Dean of Research and Development at Acharya Institute of Technology, Bengaluru, Karnataka, from 2017 onwards. His current research includes the effectiveness of 5G Green Communications, mmWave antenna design, UWB antennas, and its implementation. With 16+ years of experience in the Academic and Research field, he has published 76 research papers and eight papers submitted to IEEE Access and Reputed Book and 4 Authored Books and 3 Edited Books (CRC, ISTE, Bentham Science) with a reputed publishing house. (email: devasispradhan@acharya.ac.in).